TRAPPED MODES EMBEDDED IN THE CONTINUOUS SPECTRUM

By D. V. EVANS *and* R. PORTER

(*School of Mathematics, University of Bristol, Bristol* BS8 1TW)

SUMMARY

The existence of trapped modes due to rigid obstacles placed symmetrically in between parallel walls having either Neumann or Dirichlet conditions imposed upon them are well known to occur for frequencies below the continuous spectrum or channel cut-off and for a range of geometric configurations. In this paper, we provide convincing numerical evidence for an additional isolated trapped mode of both Neumann and Dirichlet type embedded in the continuous spectrum (or above the channel cut-off) in the case of a rigid circular cylinder placed on the centre-plane of the channel. Thus, for each type of mode we give results showing that there is just one cylinder size and wave frequency at which the trapped mode occurs.

1. Introduction

IN A RECENT paper, Maniar and Newman (**1**) showed that at particular frequencies the in-line first-order exciting forces on those cylinders near the centre of a large number of identical bottom-mounted vertical circular cylinders in a linear array become extremely large, compared to the force on an isolated cylinder. These frequencies coincide with those associated with certain trapped modes around a corresponding cylinder on the centre-plane of a wave channel. These trapped modes are of two types. The Neumann trapped modes, satisfying Neumann conditions on all solid boundaries and a Dirichlet condition on the centre-plane, were discovered by Callan *et al.* (**2**) and have been proved to exist for all values of $0 < a/d < 1$ where $2a$ is the cylinder diameter and $2d$ is the width of the channel; see Evans *et al.* (**3**). Numerical computations by Callan *et al.* (**2**) indicate that there is just one such trapped mode having a unique wavenumber, k^N, satisfying $k^N < \pi/2d$ where the angular velocity ω^N is given by $\omega^N = (gk^N \tanh k^N h)^{\frac{1}{2}}$ with h the depth of the channel. Physically the Neumann trapped mode describes an antisymmetric sloshing motion about the centre-plane of the channel which is confined to the vicinity of the cylinder and decays rapidly down the channel. Mathematically, the value $(k^N)^2$ is an eigenvalue of the Laplacian operator in the unbounded region contained between one channel wall, the centre-plane of the channel and one half of the cylinder, and $(k^N)^2$ lies below the continuous spectrum which for this problem is $[\pi^2/4d^2, \infty)$.

The second type, discovered by Maniar and Newman (**1**) and described as Dirichlet trapped modes, satisfy a Neumann condition of no normal flow through the cylinder surface but Dirichlet conditions on both the channel walls and the centre-plane. They have no obvious physical interpretation in the context of water waves in channels but are well known in the acoustical literature where they are termed acoustic

resonances. For a review, see (4). Maniar and Newman (1) used image arguments to show that both types of trapped modes would occur in the case of an infinite line of identical cylinders which explained the near resonance occurring when a large but finite line of cylinders was excited by an incident wave at the trapped mode frequency. The largest in-line forces were experienced in head seas as might be expected but the effect also occurred to a lesser extent in obliquely-incident waves.

In contrast to the Neumann trapped modes, the Dirichlet trapped modes only appear to exist for a restricted range of a/d. Thus the computations of Maniar and Newman (1) suggest that a Dirichlet trapped mode exists provided $0 < a/d \lesssim 0\cdot677$, a figure which the present authors have refined to $0\cdot6788$ using the same method. Dirichlet trapped modes also occur at higher frequencies than the Neumann modes but the corresponding trapped mode wavenumber squared satisfies $(k^D)^2 < \pi^2/d^2$. That is, it still lies below the continuous spectrum which in this case occupies $[\pi^2/d^2, \infty)$. The method used by Evans *et al.* (3) to prove the existence of a Neumann trapped mode for all $a/d \in (0, 1)$ can easily be adopted to consider the Dirichlet modes with the result that for a fairly general cross-section described by $y = \pm f(x)$ with $f(\pm a) = 0$, a Dirichlet trapped mode exists provided

$$\int_{-a}^{a} \sin(2\pi f(x)/d)\, dx > 0.$$

For the circular cylinder this reduces to $J_1(2\pi a/d) > 0$ or $a/d \lesssim 0\cdot6098$ consistent with the numerical computations.

The method employed by Callan *et al.* (2) to construct the Neumann trapped modes involved the use of appropriate multipole potentials each of which satisfied the required conditions on the centre-plane and walls of the channel and which, by restricting the allowable range of wavenumbers to lie below the lowest point of the continuous spectrum, vanished at large distances down the channel. The unknown coefficients in a sum over all such multipoles chosen to satisfy the Neumann condition on the cylinder were then shown to satisfy a real homogeneous infinite system of equations. The vanishing of the determinant of this system then provided the trapped mode frequencies. The same approach has been used by the authors (5) to determine the Dirichlet trapped modes and to confirm the results obtained by Maniar and Newman (1) who used a different method. This involved applying a general formulation valid for an arbitrary configuration of different bottom-mounted cylinders, developed by Linton and Evans (6) but which also appears in (7), to the special case of a long line of identical cylinders, assuming a phase relation between the field at adjacent cylinders consistent with an infinite line of cylinders, and using a method due to Twersky (8) to transform a slowly convergent complex infinite system to an infinite system having a real infinite determinant whose zeros can be determined relatively efficiently.

The success of the method depends on being able to reduce the generally complex system to a real one for values of wavenumber k below the cut-offs (the lowest point of the continuous spectra) $\pi/2d$ and π/d for Neumann and Dirichlet modes respectively. In contrast, the multipole method uses sets of real functions from the start and

it is clear that no waves are radiated to infinity from the multipoles for wavenumbers below the cut-off. For values above the cut-off the system is complex using either method and this is to be expected since, for example, the multipoles radiate waves down the channel which must be out of phase with the local field since net work has to be done over a cycle to radiate energy. However Maniar and Newman (1, Figs 8, 9), found that at certain wavenumbers above the cut-off, for both Neumann and Dirichlet modes (despite being complex), the modulus of the determinant of the system was extremely small, showing that only a very small energy leakage was occurring. The effect of this on a finite line of cylinders was a slight peak in the forces at those frequencies—see (1, Fig. 1).

The authors recalculated the complex determinant arising from Twersky's method and found that for a precise value of a/d and precise wavenumber the determinant is less than 10^{-9} in both the Neumann and Dirichlet cases. The implication is that these are in fact genuine trapped modes embedded in the continuous spectrum. The purpose of the present paper is to confirm this using the multipole method of Callan et al. (2). This has two advantages over the Twersky method. The complex nature of the system can be clearly seen to arise from the radiated waves from each multipole and the condition that any trapped modes should vanish at large distances can be confirmed readily from the form of construction of the solution. In contrast the behaviour at large distances is not readily available from the Twersky method which makes it difficult to confirm the required behaviour at large distances.

Extensive use is made of the paper by Callan et al. (2). The aim is to rework (2) for k lying in the range $\pi/2d < k < 3\pi/2d$ ($\pi/d < k < 2\pi/d$) for Neumann (Dirichlet) modes and show that it is possible to find a value of a/d and a corresponding k such that although each multipole separately radiates waves, it is possible to find a combination which does not, in addition to satisfying the Neumann condition on the cylinder.

2. Formulation

It follows from (2) that the velocity potential Φ for the Neumann modes can be written

$$\Phi(x, y, t) = \operatorname{Re} \phi(x, y)e^{-i\omega t}, \tag{2.1}$$

where $\phi(x, y)$ satisfies

$$(\nabla^2 + k^2)\phi = 0, \quad \text{in } r > a, \ |y| < d, \qquad r = (x^2 + y^2)^{\frac{1}{2}}, \tag{2.2}$$

$$\phi_y = 0, \quad |y| = d, \ -\infty < x < \infty, \tag{2.3}$$

$$\phi_r = 0, \quad r = a, \tag{2.4}$$

$$\phi = 0, \quad y = 0, \ |x| \geqslant a, \tag{2.5}$$

$$\phi \to 0, \quad |x| \to \infty, \ |y| \leqslant d, \tag{2.6}$$

$$\phi_x = 0, \quad x = 0, \ |y| > a. \tag{2.7}$$

Here

$$\omega^2 = gk \tanh kh. \tag{2.8}$$

In contrast to (2) we seek possible solutions of the above equations for values of k satisfying

$$\pi/2d < k < 3\pi/2d. \tag{2.9}$$

In seeking Dirichlet trapped modes we replace (2.3) by

$$\phi = 0, \qquad |y| = d, \quad -\infty < x < \infty \tag{2.10}$$

and look for possible solutions for values of k satisfying

$$\pi/d < k < 2\pi/d. \tag{2.11}$$

It is sufficient to consider $0 \leqslant y \leqslant d$ and choose functions odd in y in order to satisfy (2.5). It was shown in (2) how the fundamental singular solution $iH^{(1)}_{2n+1}(kr)\sin(2n+1)\theta$, where $r\cos\theta = x$, $r\sin\theta = y$, satisfying (2.2), (2.5) and (2.7) may be modified by including an integral term, in order to satisfy (2.3). The resulting multipole given in (2, equations (A.4), (A.5)) was shown to be purely real, and to satisfy (2.6) provided that $k < \pi/2d$. If $\pi/2d < k < 3\pi/2d$, the modifying integral term is now indeterminate, having a pole on the real path of integration. It is normal in such a case, on physical grounds, to choose a path which passes below the pole so that the now complex-valued integral behaves like a wave travelling outwards at large distances. If we do this the total multipole potential is no longer real and the resulting infinite system is complex and we would be left with the task of showing that the determinant had a real zero and that the corresponding expansion coefficients were such as to produce no waves at infinity. Instead we proceed differently, relegating showing the equivalence of the two approaches to the Appendix. The modifying integral term can also be made determinate by interpreting it as a principal value integral. This has the advantage that it remains real whilst its behaviour at large distances is now as a standing wave. Thus the resulting infinite system is also real and we have a simpler task of computing any real zeros of the real determinant which simultaneously produce a combination of standing waves which vanish at large distances.

Referring to (2, equations (A.4), (A.5)), we have for the multipoles the expressions

$$\psi_{2n+1}(r,\theta) = Y_{2n+1}\sin(2n+1)\theta$$
$$-\frac{2(-1)^n}{\pi}\int_0^\infty \frac{e^{-\gamma d}}{\cosh\gamma d}\sinh\gamma y\cos(kx\cosh v)\sinh(2n+1)v\,dv$$
$$-\frac{2}{\pi}\int_0^{\frac{1}{2}\pi}\tan\beta d\sin\beta y\cos(kx\sin u)\cos(2n+1)u\,du, \tag{2.12}$$

where $\gamma = k\sinh v$, $\beta = k\cos u$, or equivalently

$$\psi_{2n+1}(r,\theta) =$$
$$-\frac{2(-1)^n}{\pi}\int_0^\infty \frac{\cosh\gamma(d-y)}{\cosh\gamma d}\sinh\gamma y\cos(kx\cosh v)\sinh(2n+1)v\,dv$$
$$-\frac{2}{\pi}\int_0^{\frac{1}{2}\pi}\frac{\cos\beta(d-y)}{\cos\beta d}\cos(kx\sin u)\cos(2n+1)u\,du. \tag{2.13}$$

It is clear from (2.12) that (2.5) is satisfied and from (2.13) that (2.3) is satisfied. Note the single principal value in the integrals since $\pi/2d < k < 3\pi/2d$. The behaviour of $\psi_{2n+1}(r, \theta)$ for large $|x|$ can be determined from (2.13) as follows. The first integral vanishes for large $|x|$ by the Riemann–Lebesgue lemma and we can write the second as

$$I = -\frac{2}{\pi}\text{Re}\int_0^{\frac{1}{2}\pi}\frac{\cos\beta(d-y)}{\cos\beta d}e^{ikx\sin u}\cos(2n+1)u\,du. \qquad (2.14)$$

Now $\cos\beta d = 0$ when $\cos u = (2n+1)\pi/2kd$, $n = 0, \pm1,...$. But $\frac{1}{3} < \pi/2kd < 1$ so that there is just one root, $u = u_0$ say, when $n = 0$, on the path of integration. Thus

$$\beta_0 = k\cos u_0 = \pi/2d.$$

If the integral for I is now closed by a small semicircle about $u = u_0$ in the upper u-plane, the resulting complex integral is easily seen, by deforming the path slightly upwards, to vanish at $x \to \infty$, leaving a term arising from the integral around the small circle. Thus, evaluating the (half) residue,

$$I \sim -\frac{2}{\pi}\text{Re}\,\pi i\frac{\cos\beta_0(d-y)e^{ikx\sin u_0}}{kd\sin\beta_0 d\sin u_0}\cos(2n+1)u_0 \qquad \text{as } x \to \infty. \qquad (2.15)$$

For $x \to -\infty$, the integral path is closed by a semicircle in the lower half-plane with the final result, since I is even in x,

$$\psi_{2n+1}(r, \theta) \sim \frac{2\sin\beta_0 y\sin(k|x|\sin u_0)}{kd\sin u_0}\cos(2n+1)u_0, \qquad |x| \to \infty. \qquad (2.16)$$

We now seek a trapped mode in the form

$$\phi(r, \theta) = \sum_{n=0}^{\infty} k^{-1}a_n(Y'_{2n+1}(ka))^{-1}\psi_{2n+1}(r, \theta) \qquad (2.17)$$

and application of the condition (2.4) yields

$$a_m + \sum_{n=0}^{\infty} B_{mn}a_n = 0, \qquad m = 0, 1, 2,..., \qquad (2.18)$$

where $B_{mn} = A_{mn}J'_{2m+1}(ka)/Y'_{2n+1}(ka)$ as in (2). Here

$$A_{mn} = -\frac{4}{\pi}(-1)^{m+n}\int_0^{\infty}\frac{e^{-\gamma d}}{\cosh\gamma d}\sinh(2n+1)v\sinh(2m+1)v\,dv$$

$$-\frac{4}{\pi}\int_0^{\frac{1}{2}\pi}\tan\beta d\cos(2n+1)u\cos(2m+1)u\,du. \qquad (2.19)$$

Thus the system is identical to that in (2) apart from the principal value integral but we also have the requirement, from (2.16), (2.17) that

$$S = \sum_{n=0}^{\infty}\frac{a_n\cos(2n+1)u_0}{Y'_{2n+1}(ka)} = 0 \qquad (2.20)$$
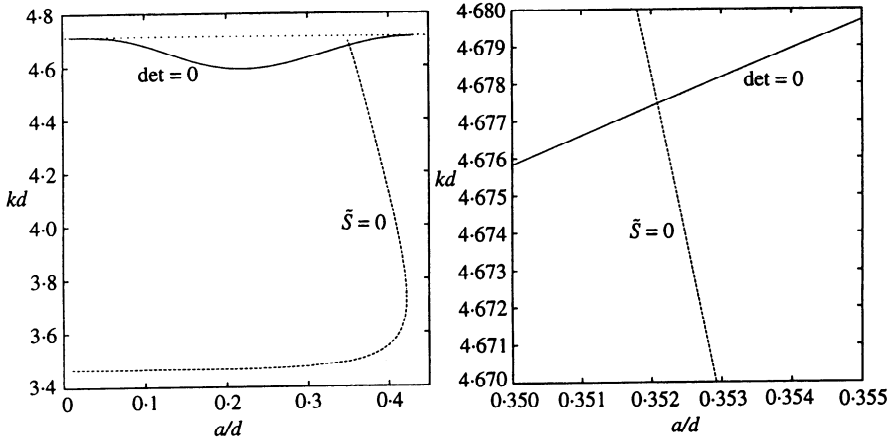
FIG. 1. Curves showing zeros of determinant and of S for the Neumann modes as functions of kd and a/d. The point of intersection is magnified in the second figure

ensuring that

$$\phi(r, \theta) \sim \frac{2S \sin \beta_0 y}{k^2 d \sin u_0} \sin(k|x| \sin u_0), \qquad |x| \to \infty \qquad (2.21)$$

satisfies condition (2.5). Once a trapped mode is found the free surface close to the cylinder is determined from

$$\phi(r, \theta) = A \sum_{n=0}^{\infty} a_n F_{2n+1}(kr) \sin(2n + 1)\theta, \qquad (2.22)$$

where

$$F_{2n+1}(kr) = \frac{J_{2n+1}(kr)}{J'_{2n+1}(ka)} - \frac{Y_{2n+1}(kr)}{Y'_{2n+1}(ka)} \qquad (2.23)$$

for any constant A and valid for $r < 2d$.

A note on the computation

The computation of the real zeros of the real determinant of the system (2.18) is straightforward, convergence to six decimal places being achieved with as few as five multipoles for the particular cylinder sizes being considered here ($a/d < \frac{1}{2}$). The principal value integral in (2.19) is of the form

$$\int_0^{\frac{1}{2}\pi} \frac{f(u)}{g(u)} \, du,$$
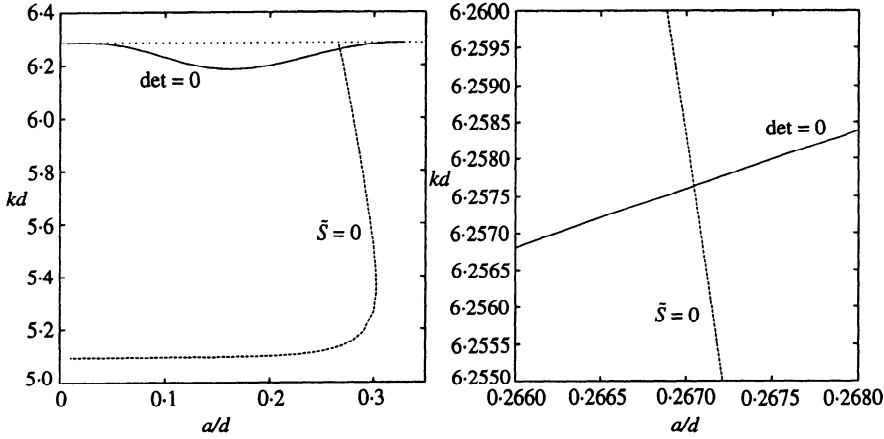
FIG. 2. Curves showing zeros of determinant and of S for the Dirichlet modes as functions of kd and a/d. The point of intersection is magnified in the second figure

where $g(u) = 0$ at $u = u_0$, $g'(u_0) \neq 0$. For $u_0 > \frac{1}{4}\pi$ we write

$$\fint_0^{\frac{1}{2}\pi} \frac{f(t)}{g(t)}\, dt = \int_0^{2u_0 - \frac{1}{2}\pi} \frac{f(t)}{g(t)}\, dt + \fint_{2u_0-\frac{1}{2}\pi}^{\frac{1}{2}\pi} \left\{ \frac{f(t)}{g(t)} - \frac{f(u_0)}{g'(u_0)(t-u_0)} \right\}\, dt, \quad (2.24)$$

where the second integral is now well-behaved and the last term in the second integral vanishes since

$$\fint_{2u_0-\frac{1}{2}\pi}^{\frac{1}{2}\pi} \frac{dt}{t - u_0} = 0.$$

For $u_0 < \frac{1}{4}\pi$ we apply a similar technique and in this case the ranges of integration in the first and second integrals on the right-hand side of (2.24) are replaced by $(2u_0, \frac{1}{2}\pi)$ and $(0, 2u_0)$ respectively.

3. Results

For $\pi/2 < kd < 3\pi/2$ we compute the values of kd for which the determinant of (2.18) vanishes as a function of a/d. Just as for values of $kd < \pi/2$, there is a unique value of kd for each a/d, and a single curve of kd versus a/d can be drawn. At each point on this curve a non-trivial vector $\mathbf{a} = \{a_0, a_1,...\}$ is defined allowing S to be computed from (2.20). Then any points on the curve of vanishing determinant for which S *also* vanishes corresponds to a trapped mode. This provides a method for determining the values of kd and a/d for which trapped modes occur. Instead, however, we choose to proceed slightly differently. The advantage of the method below will become clear later.

Let the eigenvalues of the matrix $\delta_{mn} + B_{mn}$, $m, n = 0, 1, 2,...$ in the system
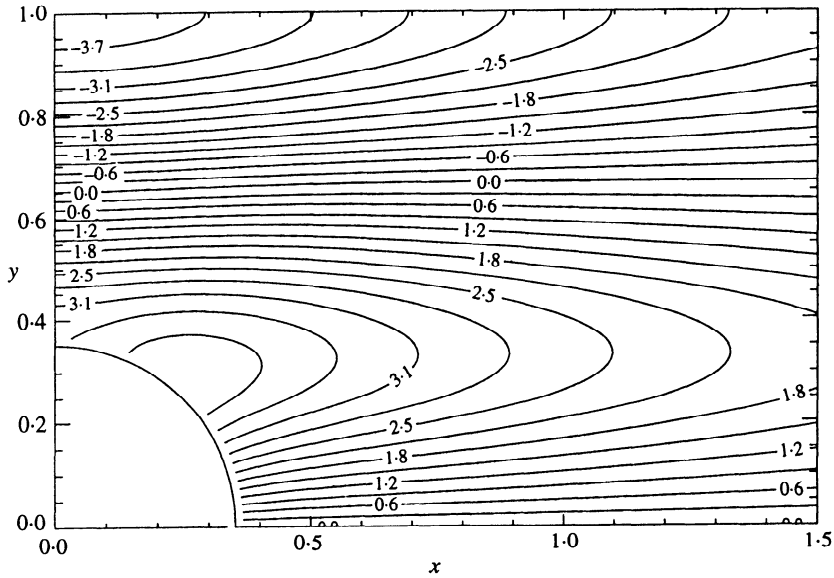
FIG. 3. Surface elevation for Neumann trapped mode

(2.18) be $\{\lambda_r\}$, each λ_r having a corresponding eigenvector $e^r = \{e_0^r, e_1^r,...\}$. Let $\lambda_m = \min_r\{|\lambda_r|\}$ and define

$$\tilde{S} = \sum_{n=0}^{\infty} \frac{e_n^m \cos(2n + 1)u_0}{Y_{2n+1}'(ka)}. \qquad (3.1)$$

Unlike S in (2.20), $\tilde{S}$ is defined over all parameters kd and a/d and not just on the curve of vanishing determinant. However, the values of S and $\tilde{S}$ do coincide on the curve of det $= 0$ where $\lambda_m = 0$, and the corresponding eigenvector e^m is equal to a. Thus, if in addition to the curve det $= 0$, the curve $\tilde{S} = 0$ is also sketched, then any points of intersection of these two curves correspond to a trapped mode. The advantage of this method is that a trapped mode is clearly seen to correspond to the crossing of two lines and that the values of kd and a/d for which a trapped mode occurs can easily be read off the graph. Moreover, as series are computed numerically by truncation and curves are not exact, it is more convincing to have two independently computed curves intersecting rather than using the information from an 'approximate' curve in a further condition that must also be satisfied.

For values of $kd \in (\pi/2, 3\pi/2)$ we plot points where $\tilde{S}$, given by (3.1) vanishes. Again this provides a unique curve of kd against a/d. The curves are shown in Fig. 1, where it can be seen that there is just one intersection indicating a trapped mode.

Increasingly refined calculations give the values at which this embedded Neumann

FIG. 4. Surface elevation for Dirichlet trapped mode

trapped mode occurs as

$$kd = 4{\cdot}677467 = 1{\cdot}488884\pi \qquad \text{and} \qquad a/d = 0{\cdot}3520905.$$

The procedure for determining the embedded Dirichlet trapped mode follows that outlined above for the Neumann modes with only minor changes arising from the replacement of (2.3) by (2.10) in the governing equations. Fundamentally this affects the form of the multipoles defined in the Neumann case by (2.12). Thus the changes for the Dirichlet case involve the replacement of $\cosh \gamma d$ by $\sinh \gamma d$ in the denominator of the first integral in (2.12) and of $\tan \beta d$ by $-\cot \beta d$ in the second. Working through with these altered expressions still gives the two equations (2.18) and (2.20) (and therefore (3.1)) but in (2.19), $\cosh \gamma d$ is replaced by $-\sinh \gamma d$ and $\tan \beta d$ is replaced by $-\cot \beta d$. Note also that now the principal value occurs at the value $u = u_0$ where $\beta_0 = k \cos u_0 = \pi/d$.

Results for the Dirichlet mode are also shown in Fig. 2 as the intersection of two curves. Precise values for this new embedded modes are

$$kd = 6{\cdot}257636 = 1{\cdot}991867\pi \qquad \text{and} \qquad a/d = 0{\cdot}2670474.$$

Contour plots of the free surface elevation near the cylinders in each case are shown in Figs 3, 4, where we have taken $d = 1$. Since there is symmetry in both $x = 0$ and $y = 0$ we only need show one quadrant of the full channel. It can be seen that in both cases the amplitude decays down the channel as required for a trapped mode and how the various boundary conditions imposed are satisfied. At a first glance it appears that in both Figs 3 and 4 there is an antinode ($\phi = 0$) parallel to the centre-

FIG. 5. Maximum exciting force on the middle cylinder in a linear array of 36 cylinders in head seas against non-dimensional wavenumber kd/π, where the cylinders have radius a and centres $2d$ apart: (a) $a/d = 0.35209$, (b) $a/d = 0.26705$

line at $y = \frac{2}{3}$ and $y = \frac{1}{2}$ respectively. However closer inspection reveals that they are in fact not straight lines and therefore cannot be replaced by parallel walls. Although the form of the trapped mode oscillation away from the cylinder resembles that of the second cross-channel eigenfunction, which in the Neumann and Dirichlet cases are $\sin 3\pi y/2d$, $\sin 2\pi y/d$ respectively, in contrast, the trapped mode solutions vanish as $|x| \to \infty$.

4. Conclusion

We have presented convincing numerical evidence for the existence of a Neumann and a Dirichlet trapped mode embedded in the continuous spectrum at just one precise value of a/d. Because in each case the value of a/d is fairly small, the corresponding wavenumber is close to the cut-off. Although the idea of embedded eigenvalues is familiar in spectral theory, it had been generally believed that they were unlikely to arise in practical situations such as that being considered here. However, the recent construction of strictly two-dimensional trapped modes embedded in

the continuous spectrum by McIver (9) using suitably positioned surface line sources illustrates the need for caution in drawing general conclusions.

That the new trapped modes described here are of practical importance is borne out by Fig. 5 which shows the effect of head seas upon the middle cylinder in a line of 36 identical cylinders spaced precisely at the required value of a/d for trapping. In addition to the peaks due to the effect of the Neumann and Dirichlet modes below their respective cut-offs, a force of approximately three times the force on an isolated cylinder is experienced at frequencies close to the new embedded Neumann and Dirichlet trapped modes. Thus in Fig. 5(a), we have chosen $a/d = 0.35209$ corresponding to the Neumann trapped mode for an infinite line of cylinders and in Fig. 5(b), $a/d = 0.26705$ is chosen to pick out the influence of the Dirichlet trapped mode solution just below $kd = 2\pi$ on the finite line of cylinders. It should be noted that the peak just below $kd = 3\pi/2$ in Fig. 5(b) is due to a small value of the complex determinant in the infinite system and termed a near-trapped mode—see (1, especially the discussion surrounding Figs 8, 9).

The authors have also adapted the approach outlined here to the problem of trapping waves above a submerged horizontal cylinder originally due to Ursell (10), again transforming a generally complex system into a real determinant system plus a constraint on the vanishing of the far field. However, they have been unable to find a trapped mode solution above the cut-off for this problem.

Acknowledgement

REFERENCES

1. H. D. MANIAR and J. N. NEWMAN, *J. Fluid Mech.* **339** (1997) 309–330.
2. M. CALLAN, C. M. LINTON and D. V. EVANS, *ibid.* **229** (1992) 51–64.
3. D. V. EVANS, M. LEVITIN and D. VASSILIEV, *ibid.* **261** (1994) 21–31.
4. R. PARKER and S. A. T. STONEMAN, *Proc. Instn mech. Engrs* **203** (1989) 9–19.
5. D. V. EVANS and R. PORTER, *J. Fluid Mech.* **339** (1997) 331–356.
6. C. M. LINTON and D. V. EVANS, *ibid.* **215** (1990) 549–569.
7. V. TWERSKY, *J. acoust. Soc. Amer.* **24** (1952) 42–46.
8. ——, *Arch. rat. Mech. Anal.* **8** (1961) 323–332.
9. M. MCIVER, *J. Fluid Mech.* **315** (1996) 257–266.
10. F. URSELL, *Proc. Camb. phil. Soc.* **47** (1951) 347–358.

APPENDIX A

Equivalence of section 2.1 *to the full complex system*

The full complex multipoles for $\pi/2d < k < 3\pi/2d$ satisfying Neumann conditions on $|y| = d$ are given by

$$\psi_{2n+1}(r, \theta) = -i H_{2n+1}(kr) \sin(2n + 1)\theta$$
$$-\frac{2(-1)^n}{\pi} \int_0^\infty \frac{e^{-\gamma d}}{\cosh \gamma d} \sinh \gamma y \cos(kx \cosh v) \sinh(2n + 1)v \, dv$$

$$+\frac{2i}{\pi}\int_0^{\frac{1}{2}\pi}\frac{e^{i\beta d}}{\cos\beta d}\sin\beta y\cos(kx\sin u)\cos(2n+1)u\,du$$

$$-\frac{2i\cos(2n+1)u_0}{kd\sin u_0}\sin\beta_0 y\cos(kx\sin u_0),\qquad\qquad\text{(A.1)}$$

where $\gamma = k\sinh v$, $\beta = k\cos u$ and $\beta_0 = k\cos u_0 = \pi/2d$. Then they describe outgoing waves at infinity:

$$\psi_{2n+1}(r,\theta)\sim-\frac{2i\cos(2n+1)u_0}{kd\sin u_0}\sin\beta_0 y e^{ik|x|\sin u_0}\qquad\text{as }|x|\to\infty.\qquad\text{(A.2)}$$

The real part of the multipoles in (A.1) is just that quoted in (2.12). Thus, we only consider the contribution of the imaginary parts of (A.1) to the final system, (2.18). So, using

$$\sin\beta y\cos(kx\sin u)=2\sum_{n=0}^{\infty}J_{2n+1}(kr)\sin(2n+1)\theta\cos(2n+1)u\qquad\text{(A.3)}$$

which can be found in (**2**, equation (A.8)) after a change of variables, we have

$$\text{Im}\{\psi_{2n+1}\}=-J_{2n+1}(kr)\sin(2n+1)\theta$$

$$+\frac{4}{\pi}\sum_{m=0}^{\infty}J_{2m+1}(kr)\sin(2m+1)\theta\int_0^{\frac{1}{2}\pi}\cos(2m+1)u\cos(2n+1)u\,du$$

$$-\frac{4\cos(2n+1)u_0}{kd\sin u_0}\sum_{m=0}^{\infty}J_{2m+1}(kr)\sin(2m+1)\theta\cos(2m+1)u_0\qquad\text{(A.4)}$$

and the first two terms cancel leaving the complex modification to A_{mn} given in (2.19) as

$$\tilde{A}_{mn}=A_{mn}-i\frac{4J'_{2m+1}(ka)\cos(2m+1)u_0\cos(2n+1)u_0}{kd\sin u_0}\qquad\text{(A.5)}$$

and the final system becomes

$$a_m+\sum_{n=0}^{\infty}B_{mn}a_n-i\left\{\frac{4J'_{2m+1}(ka)\cos(2m+1)u_0}{kd\sin u_0}\right\}S=0,\qquad m=0,1,2,...,\qquad\text{(A.6)}$$

where S is defined in (2.20) and $B_{mn}=A_{mn}J'_{2m+1}(ka)/Y'_{2n+1}(ka)$ is real. This is satisfied if and only if the real and imaginary parts are zero simultaneously. From (A.2) and (2.17) the condition that the far field vanishes for large $|x|$ reduces to $S=0$.